Journal of Statistical Physics, Vol. 53, Nos. 3/4, 1988

Fractal Patterns of Fluid Domains for Displacement Processes in Porous Media

W. G. Laidlaw,[1] G. R. Hamilton,[1] R. B. Flewwelling,[2] and W. G. Wilson[3]

Received March 16, 1988; revision received May 27, 1988

Percolation invasion displacement of a compressible defender is examined for two cases: when only the smallest accessible site is entered at each step and when all accessible sites less than the size given by a reducing back pressure are entered at each time step. Although the fractions of invading fluid are different, their scaling properties are equivalent. The effect of limited control of a back pressure in a real displacement and the effect of viscosity in a real time displacement are examined. In these cases the scaling properties of a percolation process at breakthrough are removed. As a result, one should expect that realistic displacement models will not have the singular properties usually attributed to percolation processes.

KEY WORDS: Percolation; fractal; porous; oil recovery; reservoir flooding.

1. INTRODUCTION

The displacement of one fluid by another in porous media is of considerable commercial importance—for example, in connection with oil recovery.[4] Although the majority of commercial computer models for this process are carried out at the Darcy scale[5] (where the rock structure is averaged out), a more fundamental understanding of the process can be

[1] Department of Chemistry, University of Calgary, Alberta, T1N 1N4 Canada.
[2] East Kootenay College, Cranbrook, British Columbia, Canada.
[3] Physics Department, University of Hawaii, Honolulu, Hawaii.

[4] Conventional primary production may yield only 5 to 20% of the original oil in place. Injection of the reservoir (flooding) with producer gas, with CO_2, or with water (brine) can displace another 20%. See, for example, the description of a series of carbonate reservoirs in ref. 1.

[5] See, for example, ref. 2 for a good account of the status of commercial simulators. For a discussion of the Darcy and other macroscopic models for flow in porous media, see ref. 3.

0022-4715/88/1100-0713$06.00/0

achieved by considering flow in the network of connected micrometer-scale spaces or pores of the reservoir rock. It was realized very early that pore scale flow dependend not only on locally defined physical laws but also on global properties of the pore network.[6] The availability of large-capacity fast supercomputers and the availability of microscale experiments exposing the fundamental events[6,7] has made the modeling of these processes at the pore scale a realistic goal. Several such studies, where advance is controlled by capillary force (the so-called invasion percolation model[8]) have been undertaken.[9–12] However, the applicability of the results to experiments in the laboratory or to displacement and oil recovery in the field has been questioned. In particular, any saturation calculated at a critical point such as the "breakthrough" of the gas or brine from the injector to producer well or the complete "disconnection" of the defender oil from the producer is suspect. This is because the saturations generated by percolation processes are scale dependent at these critical points. In more formal terms, the invasion domains are fractal,[13] with the unfortunate consequence that the invader saturation at breakthrough goes to zero as the system becomes infinite. This implies that the defender saturation remains at 100%, that is, 0% of the oil is "produced" even though the flood has reached the producer well.

In a computer model of the process the network of channels (throats) and spaces (pores) of a porous reservoir can be represented on a grid by, respectively, the *bonds* (i.e., the grid lines) and *sites* (i.e., the intersections of the grid lines). These bonds and sites can be given geometric properties; for example, both the cross sections r_b, r_s and the connectivity of the sites can be adjusted as appropriate for the particular porous medium.[14]

The process can then be modeled by simple rules which control the advance of fluid from an invader-occupied site to a contiguous site and withdrawal of defender fluid from this site. The physical basis for these rules could be as simple as the capillary pressure. For example, if the defender fluid (oil) is nonwetting and the invader (water) is wetting, then in every channel or pore space there is a capillary pressure in favor of an advancing water interface—one has "imbibition." Since the capillary pressure is proportional to contact angle and interfacial tension and inversely proportional to the radius of the interface, the largest capillary pressure occurs for the smallest radius, other factors being constant. Consequently, the invader fluid will have a propensity to move into the smallest contiguous defender-occupied element. The initial state of the fluid must then be characterized by a "back pressure" sufficient to prevent the invader

[6] The classic monograph of Scheidegger,[4] contains an early exposition of the connection of pore scale properties to macroscopic characteristics. Fatt[5] should receive credit for early work which treated a porous medium in terms of a network of sites and bonds.

from entering any and all of the set of sites contiguous to the invader. If we require that the radius of any site is greater than the radius of any bond (a reasonable constraint in porous rocks), this initial back pressure will be just the capillary pressure of the smallest defender-occupied site adjacent to the initial line of invader-occupied sites. This initial back pressure is taken to be insufficient to prevent penetration of the bonds. The invasion process commences by lowering the back pressure enough so that the smallest site adjacent to the invader front can be penetrated. The required pressure is directly controlled by the crosssection of the site in question, i.e., its "size," so the process is the aforementioned site-size-controlled "percolation invasion."[8]

Under the circumstances described above, an algorithm which ensures that the invader fluid is always connected to the source is a relatively trivial matter. Further, if one assumes that the defender fluid is infinitely compressible,[15] then the algorithm is further simplified and can be implemented for quite large grids. If the defender fluid is incompressible, the algorithm, although more complicated, is readily constructed[8–12] but its execution is more time-consuming. Additional complexity is introduced if, in addition to the source line, the initial state of the grid contains invader-occupied sites from a previous invasion.[16]

The purpose of this paper is not to consider more complicated algorithms, but rather to examine carefully the connection of the simple algorithms to the procedures which control invasion of a real system. We have alluded to reducing the back presure such that the single smallest accessible defender-occupied site can be invaded. What if this pressure reduction makes several smaller sites accessible? Does one imagine increasing the pressure suddenly until the smallest of this new set of sites is determined and then lowering the pressure such that only the smallest is occupied? How would a single-smallest-site process be controlled? Does one really mean penetration of the single-smallest site or is one lowering the back pressure in steps and allowing all accessible sites which are invadable at that back pressure to be invaded (ref. 8, p. 3368, paragraph b, briefly discusses this point, as does ref. 11)? If the latter "several-sites" model is invoked, what happens if the pressure can be controlled with infinite accuracy?[7] What happens if pressure control can only distinguish between site sizes which are different to two figures?[8] Does the fraction of

[7] Chen and Koplik,[17] in a carefully controlled experiment on a small (4×4) grid, argued that indeed only the smallest site was invaded if the rate was sufficiently small. Lenormand and Zarcone[18] argued that their experimental results followed the scaling laws for percolation with trapping found earlier by Wilkinson and Willemson.[8]

[8] Pressure control in the displacement experiments of Wardlaw and co-workers[6,10] is relatively crude and there is no expectation that the procedure would allow selection between two pores differing by only 1% in radius.

sites invaded at breakthrough depend in the same way on the size of the grid? Suppose the invasion process takes place at a slow but nevertheless finite velocity so that there is some viscous drag (several authors have discussed this point[19]). How would this affect the "percolation invasion" process? Modeled on a grid, this would mean that sites at different locations and with different radii could, due to viscous effects, become equal candidates for penetration. This could occur even for a very small viscous drag and would not be circumvented by an infinitely accurate pressure control. What happens to scaling properties with these changes? What happens when there is a small but position-dependent gravity field (ref. 20 examines a model where buoyancy plays a role)? We shall discover that apparently subtle details of the implementation of the algorithm may profoundly affect the properties of the invasion, especially scaling properties near the critical point.

Because of its central role, we begin by examining the single-site conventional percolation invasion model of Wilkinson and Willemsen.[8] This process yields a fractal object at breakthrough and will be compared to the more realistic model where several sites can be simultaneously occupied. We will give a proof that this latter process leads to the same fractal dimension as the single-site model. The examination of the physical control of the several-site model suggests a variety of means to relax the mathematical model which will violate the fundamental criteria required for the fractal character of a percolation process. Finally, we cite numerical measurements of the dimension for the algorithms appropriate to each of these models.

2. PERCOLATION INVASION

We consider a grid in two dimensions, of width L and length $2L$, with sites labeled $L_{i,j}$, where $1 \leqslant i \leqslant L$, $1 \leqslant j \leqslant 2L$. The source (injector) of the invader fluid is the line of sites $L_{i,1}$ $(1 \leqslant i \leqslant L)$ and the sink (producer) is a line of sites $L_{i,2L}$ $(1 \leqslant i \leqslant L)$. The edges $L_{1,j}$ and $L_{L,j}$ are neighbors (i.e., as on a cylinder). Sites on the grid are assigned "sizes" $(0 \leqslant r_{ij} \leqslant 1)$ selected at random from a uniform distribution and each site is connected to four neighbors. The initial state has all sites of the source line occupied by the invading phase and all remaining sites occupied by a defending phase, which is taken to be infinitely compressible.[9]

[9] The use of an infinitely compressible phase is not as unphysical as might appear at first. If the disconnected phase is wetting, the disconnection may not be sufficient to rupture the thin film adhering to the walls of the system and as pressure is increased the apparently trapped fluid may leak away. See, for example, Lenormand.[15]

2.1. The "Control Volume" or "Single-Site" Process

In the algorithm for the percolation invasion process, one seeks the smallest size defender-occupied site contiguous to the invader front (i.e., initially one would test all sites L_{i2}, $1 \leqslant i \leqslant L$, and seek the smallest). Once this single smallest site is identified, it is occupied by the invader. This step creates additional sites contiguous to the invader and the set of all sites contiguous to the invader are again examined for the smallest size and when it is found this single site is invaded. One site at a time is invaded, each with its own capillary pressure. Consequently, control of this process would require a rapidly oscillating back pressure rather than a monotonically decreasing pressure. However, one could imagine carefully controlling the available volume of invader such that only one site at a time is penetrated, with the presumption that this would be the smallest site. The process terminates when a single site on the sink line is penetrated by the invader—this is called breakthrough.

For any particular grid the invasion process will have resulted in the occupation of one site which is larger than all other sites in the invader domain. We let this site be located at X_C, Y_C and let the size of the site be denoted as R_C. The capillary pressure associated with a fluid interface in this site is P_C and is proportional to $1/R_C$.

At breakthrough, there is a continuous (i.e., from source to sink) invader domain constituted by all sites which are occupied by the invader. The number of sites in this domain divided by the total number of sites in the grid is the percent continuous-invader-at-breakthrough (%CIBT). Similarly, a number of sites occupied by a defender will have been surrounded by the invader and hence cutoff or disconnected from the sink. This number yields a percent disconnected-defender-at-breakthrough (%DDBT). Depending on boundary effects, one also has some defender near the sink "end" of the grid which is neither disconnected not displaced and is referred to as percent connected-defender-at-breakthrough (%CDBT).

Although the grids over which the invasion process takes place are constructed such that the sizes of the sites are "random," it is nevertheless true that any particular realization is different in its details. Consequently, the position of the critical site in any particular grid may be anywhere in the grid, i.e., $1 \leqslant X_C \leqslant L_X$, $1 \leqslant Y_C \leqslant L_Y$. Since all values of X_C from 1 to L_X are equally probable, the average value of $X_C = \langle X_c \rangle$ over a large number of realizations of the grid would be $\langle X_c \rangle \equiv x_c = L_X/2$ and $\langle Y_c \rangle \equiv y_c = L_Y/2$. If the site sizes for any grid are ordered from smallest to largest (i.e., $R_{\min}$ to $R_{\max}$) then, for any particular grid, R_C will lie at some particular position in this ordered set. Indeed it can be "shown" that the

average value of R_C over a large number of grids is such that 59.28% of the sites are smaller than R_C.[10] Consequently, if one sets the largest site to unity, then, for a uniform distribution of sizes, the critical fractional size is $R_C = 0.5928$. We should emphasize that a value such as 0.5928 is the value for infinitely large grids, and for finite-size grids one should say that R_C approaches 0.5928. Rather than refer to averages over many grids, we shall henceforth refer to an "average grid" in which the critical fractional size is 0.5928, located at the midpoint $x_c = L_X/2$, $y_c = L_Y/2$, and for which the percentage of sites occupied by defender at breakthrough in this average grid is denoted by $\langle \%\text{CIBT} \rangle$. Similarly, we will have an average percentage disconnected defender $\langle \%\text{DDBT} \rangle$.

Since for percolation invasion the invader domain at breakthrough is known to be a fractal object with dimension $D = 1.896$,[11] its density, which is just $\langle \%\text{CIBT} \rangle$, will scale as[13]

$$\langle \%\text{CIBT} \rangle = CL^{D-2} = CL^{-0.104} \tag{1}$$

where C is a constant. As $L \to \infty$ the average percent invader at breakthrough will go to zero. Thus, the control-volume percolation invasion algorithm leads to a saturation which is scale dependent at the breakthrough point. This is definitely an undesirable feature if one wishes to apply the results to real systems of arbitrary size.

2.2. The "Control-Pressure" or "Several-Sites" Process

As an alternative to the "control-volume" invasion percolation process (CV) described above, one could consider a "control-pressure" invasion process (CP). The first step in the imbibition process is now to ascertain whether any of the defender-occupied sites L_{i2} $(1 \leqslant i \leqslant L)$, contiguous to the invader, are smaller than some selected size. For example, one could start with a size 0.01 (which is equivalent to a large capillary pressure, in turn requiring a large "back pressure" to hold the imbibing liquid in check), allowing *all* sites L_{i2} $(1 \leqslant i \leqslant L)$ contiguous to the invader and with size equal to or less than 0.01 to be penetrated. There could be several such sites! The invasion creates additional boundary sites and these new sites are examined to see if any of them are of a size equal to or less than the currently selected size of 0.01, and if so, they are penetrated. The process is

[10] There is a substantial literature on percolation thresholds, both "experimental" (computer simulations) and "theoretical" (e.g., Bethe trees).[21] For a recent simulation result see ref. 22 and for a theoretical analysis see ref. 23.

[11] Stauffer[24] remarks that "two dimensional exponents are widely believed to be exact" (p. 96), and gives $D = 91/48 \simeq 1.896$. See also refs. 25.

repeated until no further advance is possible at the selected size. The size is then increased slightly, for example, to 0.02 (i.e., the back pressure is decreased appropriately) and all sites on the boundary of size equal to or less than 0.02 are penetrated and the search is continued until again no further advance is possible at the selected size. The process achieves breakthrough when the size selected (i.e., back pressure selected) allows at least one site on the sink line to be penetrated (it should be emphasized that this last pressure reduction could allow several sites on the sink line to be penetrated, since *all* contiguous sites of size equal to or less than the breakthrough size are penetrated in this final step).

As with the CV process, there exists a single largest site R'_C through which the invader in the CP process must pass in order to achieve breakthrough. The position of this site is located at X'_c, Y'_c, where the primes indicate that, at this point in the argument, we have not proved that the site in question is the same as for the CV process.

2.3. Comparison of the CV and CP Patterns

2.3.1. Just As the Critical Size Is Encountered. In the CV process the algorithm seeks only the smallest site, and so, as the invader cluster "grows," the size of single new growth sites may be smaller or larger than any site opened up by the previous growth step. In effect, the sizes of the sites invaded increase or decrease as the "easiest path" is sought, until eventually the size R_C is encountered. The location of the site being invaded may be anywhere on the front. Certainly, just before the CV process encounters the critical size R_C at x_C, y_C it will have probed *all* sites with size smaller than R_C which are connected to the seeding line by invading fluid. We can illustrate schematically the invaded region as in Fig. 1, where c indicates "dead-end" regions which terminated at sites with sizes greater than R_C and where b_1 is a region that contains R_C on its boundary (regions c and b_1 are connected only through the source line). All sites with size $R < R_C$ which are accessible from the seed line will have been penetrated by an invader.

For the CP algorithm, invasion begins by inquiring whether sites accessible to the front are less than a chosen control size (i.e., equivalent to a chosen control pressure). Sites of many different sizes (all less than the control size) are penetrated at this point. Then the control size is increased and further advance permitted. Consequently, at each control size a group of sizes (all less than the control size) are entered. The largest size in each group does, however, show a steady increase as the control size is increased. Eventually the control size increase to R_C, at which point all sites with size less than R_C and which are connected to the seed line will

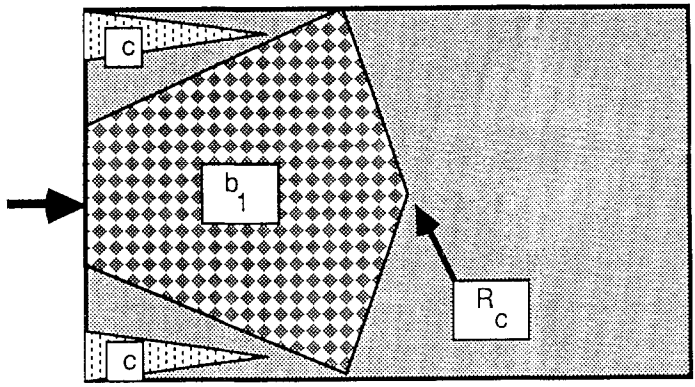

Fig. 1. Pattern of invaded sites just as the critical pore is reached. Sites which will be part of a continuous cluster, b_1. Sites which are part of a "dead-end" cluster, c. Sites which have not yet been invaded are the remaining regions.

have been invaded. Regions c and b_2 analogous to the CV case could be defined and they are in fact the same regions as c and b_1. The order in which these sites were invaded is different in the two cases, but as long as the defender is compressible the invaded regions c and b_1 in Fig. 1 are the same for both CV and CP.

2.3.2. The Density at Breakthrough. From the critical point forward the results for the two algorithms do differ. The CV process seeks the easiest path forward and consequently need only enter such sites as are necessary to generate a connected path from X_C, Y_C to breakthrough. In the CP process *all* sites connected to the source by an invader and which are less than R_C will be penetrated as the invasion front proceeds to breakthrough. The distinction between the two processes is illustrated in Fig. 2, and in Figs. 3a and 3b the completed patterns are compared schematically.

Since many more sites are occupied by CP in the last stage of invasion, the region a_2 in Fig. 3b covers more sites than its analog a_1 in Fig. 3a. The density of the CP pattern,

$$\langle \%\text{CIBT} \rangle' = (c + b_1) + a_2 \tag{2}$$

is greater than or equal to that for CV

$$\langle \%\text{CIBT} \rangle = (c + b_1) + a_1 \tag{3}$$

Since $\langle \%\text{CIBT} \rangle$ for the CV process goes to zero as $L \to \infty$, it is clear that *each* of a_1, b_1, and c go to zero. But the scaling properties of the invader

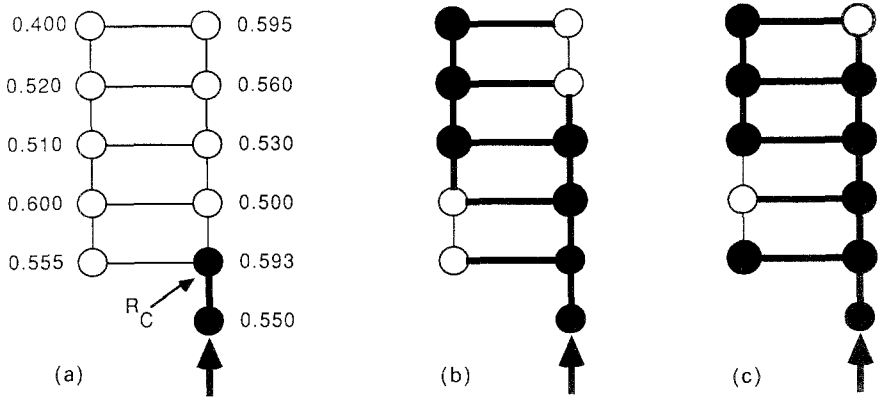

Fig. 2. Pore scale patterns: (a) pore sizes; (b) volume control (easiest path); (c) pressure control (possible path).

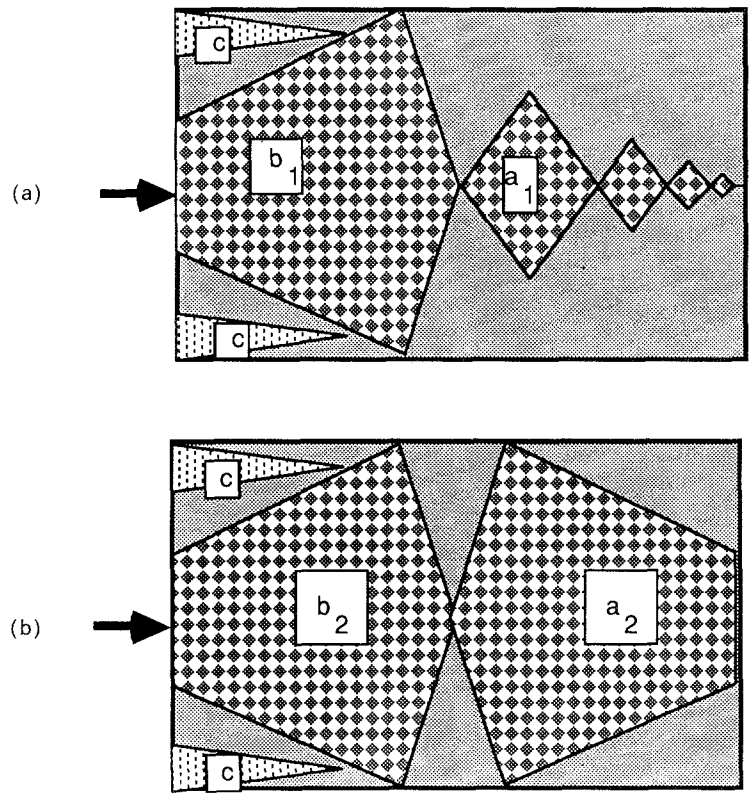

Fig. 3. Schematic pattern: (a) volume control; (b) pressure control.

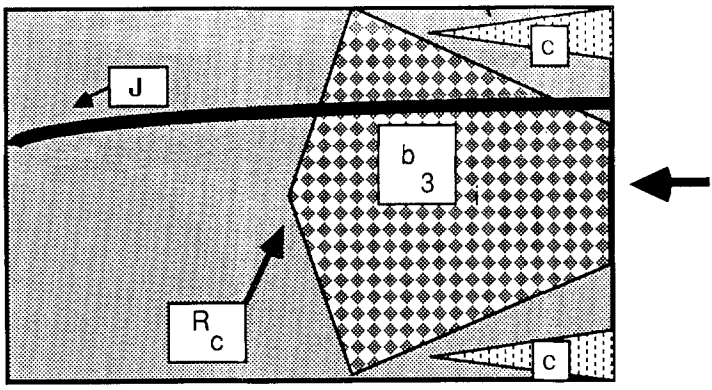

Fig. 4. A reverse path: invasion from the opposite end just before the critical pore is reached; hypothetical path, J.

fraction $\langle \%\text{CIBT} \rangle$ for CP are not fully established, for the scaling properties of a_2 must still be investigated.

2.3.3. A Reverse Process. To investigate the scaling of a_2, we consider the same grid used heretofore except that the invasion process begins from the opposite "end." The CP process results in the invasion of the regions denoted by c and b_3 in Fig. 4. We assert that the region b_3 terminates at the same critical site as b_1 and continues on to breakthrough, generating a_3 as it does so (cf. Fig. 5). In order to check the validity of this assertion, consider an alternative breakthrough path that does not include the same R_C. A path starting anywhere along the line $x = L_x$, $1 \leqslant L_y \leqslant L_x$, such as J in Fig. 4 would of course terminate somewhere on the line

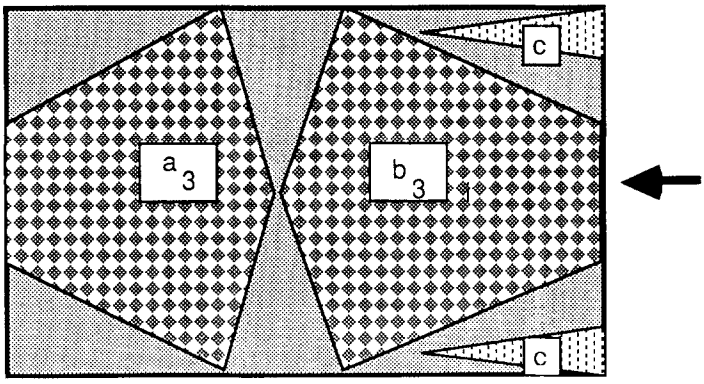

Fig. 5. A reverse path: invasion from opposite end.

$x = 1$, $1 \leqslant y \leqslant L_y$, i.e., it would connect to the seed line. The existence of such a path would be ruled out, since by construction (recall Section 1.2) at breakthrough, any path from the left boundary to the right boundary must include the site of size R_C at X_c, Y_c. Consequently, the path J does not exist, i.e., all paths must include R_C at X_C, Y_C—thus $R'_C = R_C$ and $X'_C = X_C$, $Y'_C = Y_C$. Since this is true, one can construct Fig. 5, where it is clear that $b_3 = b_2$.

Further, since there is nothing unique about which "end" of the average grid one starts from, it is evident that $a_3 = a_2$ and $b_3 = b_2$. Hence, $b_1 = b_2 = b_3 = a_3 = a_2$. Since one knows the scaling properties of b_1, namely, as $L \to \infty$, $b_1 \to 0$, then one now knows that $a_2 \to 0$ also. Our conclusion is that even though the CP invasion process generates a more robust invasion pattern than CV (cf. Figs. 2 and 3), it nevertheless scales with L with an identical fractal dimension, and for infinitely large grids $\langle \%\text{CIBT} \rangle'$ also goes to zero.

2.3.4. Comparison of the Fractal Dimension Obtained for CV and CP by a Simulation. In order to illustrate these features we present in Fig. 6 the results of calculations for the invasion process for the CV and CP algorithms for $2L \times L$ grids of increasing size. In every case the measurements were over the central $L \times L$ domain (from $L/4$ to $3L/4$) and at least 500 realizations were made for each size L except the last two, where 250 realizations were obtained. The standard error of the invader fractions is ± 0.001. For $L \geqslant 64$, Fig. 6 shows the same linear decay of $\langle \%\text{CIBT} \rangle$ for both CV and CP. The slope indicates a fractal dimension of about 1.89.

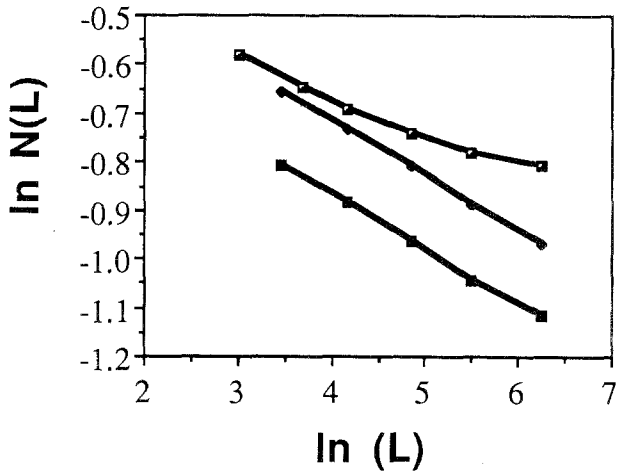

Fig. 6. Fraction of sites occupied by continuous invader N vs. size of the grid L.

In support of this result we have also calculated the dimension D_m directly on the largest grid (1024×512), using the expression[26]

$$D_m(\mathrm{CI}) = \frac{\ln(N(l_m))/N(l_{m+1})}{\ln(l_{m+1}/l_m)} \tag{4}$$

where (4) $N(l_m)$ is the number of times a window of size $l_m = 2^m$ must be laid down to cover the invader-occupied sites on the grid. Using Eq. (4) and an extrapolation technique,[12] the best values of $D(\mathrm{CI})$ are 1.89 for CV and 1.90 for CP, both of which are close to the accepted value of 1.896.[21-23]

3. REALIZATION OF THE CRITICAL POINT: LIMITATIONS

The arguments of Section 2 have relied on a grid in which no two sites have the same size—a requirement realized only when each site is given to infinite accuracy. Further, the algorithm is presumed to be capable of infinite accuracy in making comparisons of sizes of sites. These requirements allow one to assert that a *single* critical size exists and that the algorithm will find this site precisely. If this criterion is not fulfilled, then the arguments of the previous sections fail.

Suppose the accuracy of the back pressure is limited. For example, in an imbibition process, suppose that the control of back pressure is only such that the control size must be increased by increments of 0.01 rather than an infinitesmal amount. As the control size is increased from 0.59 to 0.60 in the CP invasion process on an infinite grid one must overshoot the critical size by $0.6000 - 0.5928 = 0.0072$ to achieve breakthrough and for a finite grid such as 512×256 one will, on average, exceed R_c by about 0.005. A schematic representation of the pattern at breakthrough is given in Fig. 7. The invader fractions recorded as "breakthrough" are not the same as those of breakthrough for the algorithm with infinite accuracy and will, in consequence, have different scaling properties. Indeed, as soon as the critical point is passed, the Hausdorff dimension will be exactly 2 for an infinite grid and tend to 2 for a finite grid.[28] The invader fraction no longer scales to zero with L according to Eq. (1). Thus, only an infinitely accurate pressure would ensure that the fractal properties of the idealized CP process were realized.

Suppose the invasion process takes place over a finite length of time. The viscous drag will result in both a change in the value of the critical size

[12] See ref. 26 for details of our method. For the use of extrapolations in determining critical parameters see ref. 27.

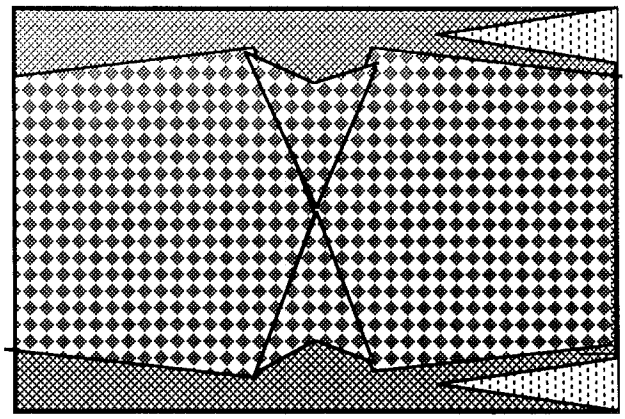

Fig. 7. Pressure control (relaxed), CPR.

and a shift in the location of the critical size away from the position characteristic of the fractal pattern of the exact CP algorithm. Due to the viscous drag, the external back pressure required to prohibit invasion of a "downstream" site could be less than for an "upstream" site even though the downstream site were smaller. Consequently, viscous drag could be viewed as changing the effective size of the grid sites in a systematic way.

As an illustration, consider the sketch in Fig. 8, where a grid has been divided into three equal infinite regions with a size bias which has reduced the site sizes by 0.000, 0.010, and 0.020 in, respectively, regions A, B, and C. In order that breakthrough occur for region A, the back pressure must be reduced to allow the penetration of sizes of up to 0.593 or $p_c^A = \alpha/0.593$ (here α is a constant characteristic of the interfacial tension and the contact angle). In order to break through region B, the back pressure would have to be reduced to allow penetration of sizes of up to $0.593 - 0.010 = 0.583$, i.e., $p_c^B = \alpha/0.583$, and for region C one would have $p_c^C = \alpha/0.573$. Since breakthrough for the entire grid requires passage through all three regions, one would have to reduce the back pressure to at least p_c^A. In so doing, one has reduced it more than required for regions B and C and in these regions the critical size would be exceeded by, respectively, 0.01 and 0.02. Thus, one expects the dimension of the invading fluid for regions B and C to be two rather than 1.896—the dimension of a percolating cluster at breakthrough. Since regions B and C represent a finite fraction of the grid, the density of the invading cluster will not scale to zero as the size L of the grid goes to infinity.

For clarity of exposition, the size reductions in regions A, B, and C above were discrete. However, provided the size reduction function $f(X)$ is

a continuous, monotonically decreasing function with finite slope at $X = 0$, then the location of the critical point will approach the source line and the critical size will approach $0.593 + f(X = 0)$.

If the process requires a positive size bias, similar arguments apply. The most difficult region to penetrate will now approach the sink line and reduction of the back pressure to allow penetration of this region will exceed that required for upstream regions. Consequently, the Haussdorff dimension for regions A and B will be 2 for an infinite grid (and will approach 2 for a finite grid) and the density of the invader taken over the entire grid will not scale to zero as the grid size is increased. As with the previous case, only now for a monotonically increasing function $f(X)$, the

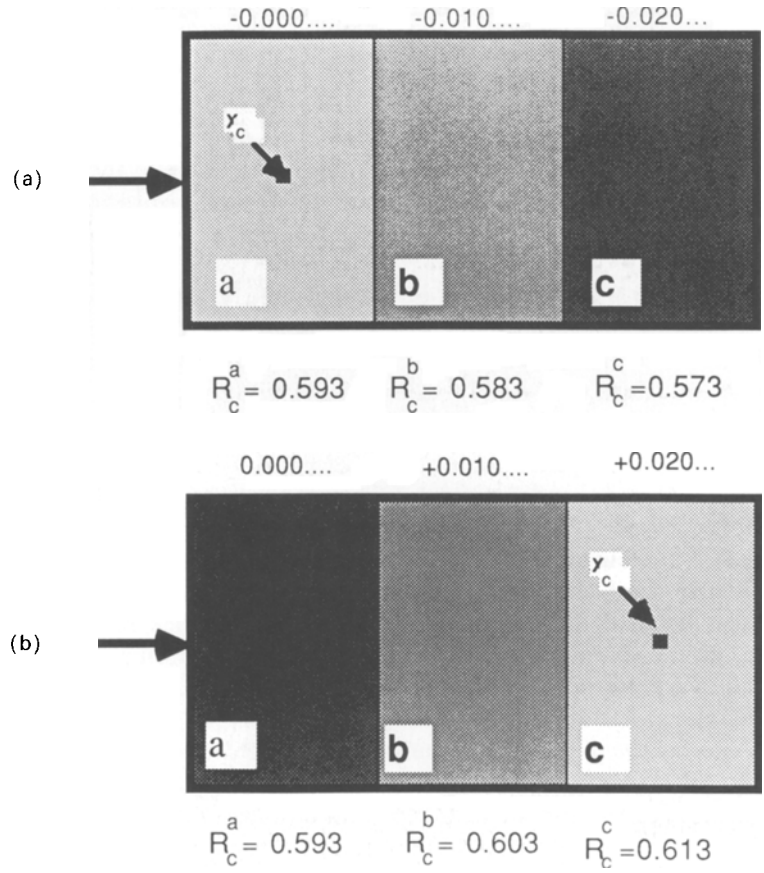

Fig. 8. (a) Effect of negative size bias on critical size. (b) Effect of positive size bias on critical size.

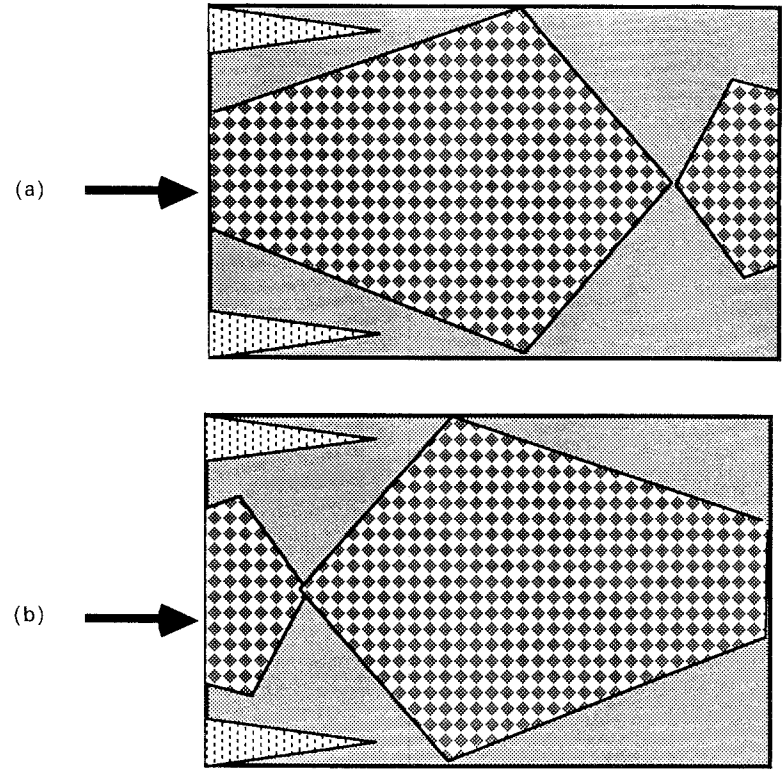

Fig. 9. (a) Pressure gradient, $B > 0$, due to viscosity or gravity. (b) Pressure gradient, $B < 0$, due to viscosity or gravity.

location of the critical size will approach the sink line and the critical size will approach $0.593 + f(X = 2L)$.

Schematic representations of the patterns due to a positive and negative site size bias are given in Fig. 9. The invader-occupied sites are not the same as those of the exact CP algorithm. Only an infinitely slow process will ensure that the fractal properties of the percolation process are realized. The fractal dimension and saturations appropriate to a specific model are given in Section 4.2.

4. APPLICATION: TOWARD MORE REALISTIC INVASION ALGORITHMS

These two illustrations should serve to make it clear that not all invasion processes and not all simulations should presume a well-determined "critical site." Nor should one expect fractal properties for all

displacement processes on a grid. Indeed, one might assert that a more realistic model of an invasion process would not be infinitely slow nor would there be infinite accuracy to the pressure control.

4.1. Limited Pressure Control

A simple way to model this is to presume a limited accuracy in the algorithm—a feature readily available in the CP process. Consequently, we shall refer to the constant-pressure (CP) process as CPX when there is a single critical site which can be distinguished from all others by precise (exact) control of the back pressure, and we shall refer to a constant-pressure process as CPR when the requirements for a unique critical point are relaxed ($\equiv$R) by, for example, citing sizes (or pressures) to a finite accuracy, e.g., CPR(0.01) denotes an algorithm in which sizes are compared to only two decimals.

For the CPR algorithm, e.g., CP(0.01), the process can be implemented by finding the critical size for a given grid and then stepping up to a size 0.01 larger. Alternatively the CPR algorithm can be implemented by increasing the size in steps of 0.01 from 0.58 to 0.59 to 0.60 and hence exceed the critical size 0.593 by, on average about 0.005 [this would be denoted CP(0.005)]. As Fig. 6 indicates, the curve for $\ln\langle\%\text{CIBT}\rangle$, for the finite accuracy CP(0.005) algorithm, flattens out to a constant value, as one would expect if the dimension approaches 2. A direct calculation of the dimension for the 512×256 grid using Eq. (4) shows that the dimension of the continuous invader (CI) does indeed approach 2 as the accuracy of the control is relaxed. For example, for CP(0.001), $D \simeq 1.91$; for CP(0.01), $D \simeq 1.95$; and for CP(0.02), $D \simeq 1.98$. Further, for CP(0.02), the extrapolated value (see footnote 12) of D(CI) is at least 1.99. Of course, for an infinite grid, the CPR algorithm will yield a D of precisely 2.

4.2. A Pressure Gradient Bias (Viscous Drag)

In order to give more substance to the role of viscosity, we consider a simple model in which the viscous drag of the moving fluid is associated with the length x of the moving column of invader and the length $L-x$ of the moving column of the defender. Thus, the viscous drag is

$$f_{\text{visc}} = \mu_{\text{I}} x + \mu_{\text{D}}(L-x) \tag{5}$$

where μ_{I} and μ_{D} are effective viscosities associated with movement of

invader and defender fluids, respectively. Introducing the viscosity ratio $U = \mu_D/\mu_I$, one has

$$f_{visc} = \mu_I[UL_x + (1-U)\,x] \tag{6}$$

Clearly, μ_I scales the viscous drag for the system and in that sense is a measure of the velocity of the displacement process. On the other hand, $[UL_x + (1-U)_x]$ indicates the change in drag as the composition of the fluid "column" changes with displacement of the front and is of course dependent on the viscosity ratio U and on x.

A viscosity ratio of $U = 10$ is not unreasonable for water displacing oil and under these circumstances viscous drag will be much larger at the beginning of the displacement [e.g., $f_{visc}(x=0) = \mu_I UL_x$], whereas at the end the viscous drag is much less [e.g., $f_{visc}(x=L_x) = \mu_I L_x$]. Thus, the back pressure required to keep the invader out of a site of given size will be less than without the viscous drag. In other words, the drag at every site reduces the ability of capillary pressure to cause the advance of the invader. This is equivalent to increasing the effective size of every site over and above the size given by the random number generator which defined the grid sizes. Thus, the effective size can have a constant term [cf. the term $\mu_I \mu L_x$ in Eq. (6)], which we denote as B_0. The effective size may also be controlled by a systematic component, denoted as Bx [cf. the term $\mu_I(1-U)\,x$ in Eq. (6)], so that the effective size will change as one moves down the grid. For the case $U > 1$ the drag decreases as x increases, so that the initial increase in size B_0 will be reduced by the value of $(B)\,x$. Thus, the effective radius of the site is just

$$r_{site}^{effective} = r_{site} + B_0 - Bx, \qquad \text{where} \quad B > 0 \text{ if } U > 1 \tag{7}$$

In order for advance, the site in question must generate a capillary pressure greater than the back pressure which controls advance. In other words, the effective size of the site must be less than the control size which would generate a cap pressure equivalent to the control back pressure,

$$r_{size}^{effective} \leqslant r_{control} \tag{8}$$

A displacement process taking into account viscous drag was invoked using Eqs. (7) and (8) in the CV and in the CPX algorithms. Two hundred realizations on a 256×128 grid were obtained and the results are displayed in Table I. In all cases the constant term B_0 was set to zero and to illustrate the effect of a stabilizing viscosity ratio $U > 1$ and a destabilizing viscosity ratio $U < 1$ both a positive and a negative bias were employed. As the entries in the table show, the $\langle$%CIBT$\rangle$ is essentially the same (58.5% and 58.9%) for either bias when the CPX algorithm is used, whereas for CV

Table I. Effect of Viscous Drag on an Invasion Percolation Process on a 256×128 Grid

Value of B in Eq. (7)		−0.0018	0	+0.0018
Position of Critical Site		40	128	218
CV	⟨%CIBT⟩	23.1	38.8	58.7
	D(CI)	1.75	1.89	>1.95
CPX	⟨%CIBT⟩	58.5	44.5	58.9
	D(CI)	>1.98	1.90	>1.96

they are significantly different (23.1% and 58.7%). This is because of the inherent asymmetry of the CV process (see Fig. 3). As one might expect, the location of the critical site is shifted from the midpoint (128) downstream to 218 for the positive bias and upstream to 40 for the negative bias. The fractal dimension D(CI) of the continuous invader, measured using Eq. (4) and our extrapolation technique,[26] approaches 2 for the CPX algorithm for either bias on a finite grid (it is >1.98 for a 512×256 grid with $B = 0.009$) and would be 2 for an infinite grid. Consequently, the viscous drag tends to increase the dimension for a CPX algorithm and produce an invasion density which does not scale to zero as the grid size becomes infinite.

5. CONCLUDING REMARKS

The CP percolation process, in which a compressible defender is displaced simultaneously at several sites, has the same fractal dimension as the CV process in which only a single site at a time is invaded. The advantage of the CP process is that it is easy to parametrize the control mechanism as a "back pressure" and consequently one can make an intelligent assessment of the accuracy of this control. We have argued that in a real model one cannot realistically expect the infinite accuracy implied by the CP algorithm, and consequently realistic computer models should incorporate this limitation. We have shown that a relaxation of the CP algorithm will subvert the properties of the process required for scale-dependent densities. Consequently, one should expect that a realistic model of the displacement process will not exhibit the scaling properties associated with an idealized percolation process on an infinite grid.

ACKNOWLEDGMENTS

The support of the National Science and Engineering Research Council of Canada is gratefully acknowledged, as is the support of one of

us (G.R.H.) by the Government of Canada SEED program. This work received its initial stimulus from efforts of N. C. Wardlaw and Li Yu to apply their micromodel results for porous media and has benefited from continuing discussions with them and with R. Maier. One of the authors (W.G.L.) would also wish to acknowledge the stimulus for this work provided by P. P. Crooker.

REFERENCES

1. D. Jardine and J. W. Wilshart, Society of Petroleum Engineering Technical Papers SPE# 10010 (1982), Microfiche **82**:9.
2. K. Aziz and A. Settari, *Petroleum Reservoir Simulation* (Applied Science, London, 1979).
3. C. M. Marle, *Multiphase Flow in Porous Media* (Gulf Publishing Company, 1981).
4. A. E. Scheidegger, *Physics of Flow Through Porous Media* (University of Toronto Press, 1974).
5. I. Fatt, *Petr. Trans. AIME* **207**:114–181 (1956).
6. Li Yu and N. C. Wardlaw, *J. Colloid Interface Sci.* **109**:461, 473 (1986).
7. R. Lenormand, C. Zarcone, and A. Sarr, *J. Fluid Mech.* **35**:337 (1983).
8. D. Wilkinson and J. F. Willemsen, *J. Phys.* **16A**:3365 (1983).
9. K. K. Mohanty and S. J. Salter, Society of Petroleum Engineering Technical Papers SPE #11017.
10. Li Yu, W. G. Laidlaw, and N. C. Wardlaw, *Adv. Colloid Interface Sci.* **26**:1–68 (1986).
11. M. Dias and D. Wilkinson, *J. Phys. A* **19**:3131 (1986).
12. M. Dias and . Piatakes, *J. Fluid Mech.* **164**:305 (1986).
13. R. Orbach, *Science* **231**:814 (1986).
14. M. Yanuka, F. A. L. Dulien, and D. E. Elrick, *J. Colloid Interface Sci.* **112**:24 (1986).
15. R. Lenormand, *Physica* **140A**:114 (1986).
16. R. Maier, Ph. D. Thesis, Chemistry Department, University of Calgary, Calgary, Alberta, Canada (1988).
17. J. D. Chen and J. Koplik, *J. Collloid Interface Sci.* **108**:304 (1985).
18. R. Lenormand and C. Zarcone, *Phys. Rev. Lett.* **54**:2226 (1985).
19. Lenormand, *Physica* **140A**:114 (1986); P. R. King, *J. Phys. A* **20**:L259 (1987); G. Daccord, J. Nittmann, and H. E. Stanley, in *On Growth and Form*, H. E. Stanley and N. Ostrowsky, eds. (Nijhoff, 1986), p. 203.
20. D. Wilkinson, *Phys. Rev. A* **30**:520 (1984).
21. M. Sahimi, in *The Mathematics and Physics of Disordered Media* B. D. Hughes and B. W. Ninham, eds., pp. 314–346.
22. D. Wilkinson and M. Barsony, *J. Phys. A Math. Gen.* **17L**:129 (1984).
23. B. Nickel and D. Wilkinson, *Phys. Rev. Lett.* **51**:71 (1983).
24. D. Stauffer, in *On Growth and Form*, H. E. Stanley and N. Ostrowsky, eds. (Nijhoff, 1986), p. 78.
25. R. Pearson, *Phys. Rev. B* **22**:2579 (1980); M. Den Nijs, *J. Phys. A Math. Gen.* **12**:1857 (1979).
26. G. R. Hamilton, W. G. Laidlaw, R. B. Flewelling, and R. Maier, to be published.
27. K. M. Middlemiss, S. G. Whittington, and D. S. Gaunt, *J. Phys. A* **13**:1835 (1980).
28. D. Stauffer, *Introduction to Percolation Theory* (Taylor and Francis, 1985), p. 65, Eq. (51).